Int. J. Solids Structures Vol. 27, No. 1, pp. 73–87, 1991
Printed in Great Britain

0020–7683/91 $3.00 + .00
© 1990 Pergamon Press plc

AXISYMMETRIC INDENTATION OF AN ELASTIC LAYER SUPPORTED BY A WINKLER FOUNDATION

J. P. DEMPSEY, Z. G. ZHAO and H. LI
Department of Civil and Environmental Engineering, Clarkson University, Potsdam, NY 13676, U.S.A.

(*Received* 15 *August* 1989; *in revised form* 30 *October* 1989)

Abstract—Axisymmetric indentation problems of an elastic layer supported by a Winkler foundation are studied in this paper. The indentation on the upper surface is made by a rigid axisymmetric conical, paraboloidal or ellipsoidal indenter. Fundamental solutions for an arbitrary surface load are derived first. The above problems are formulated into an integral equation which is solved numerically. Extensive results are provided for contact radii, displacements and contact pressures. A layer on a rigid smooth base is treated as a special case of the Winkler foundation. The associated analytical solutions for the rigid indenters on a half space are retrieved as the layer depth approaches infinity. Conversely, useful relations are also derived from thin plate theory for relatively shallow layers.

INTRODUCTION

Axisymmetric contact of an elastic, homogeneous and isotropic layer supported by a Winkler foundation is studied in this paper. The elastic layer has a finite depth and infinite in-plane dimensions. The upper surface of the layer is subjected to axisymmetric deformations imposed by a rigid conical, paraboloidal or ellipsoidal indenter. The contact is tensionless and frictionless. Prior to treating these particular applications, the fundamental full-field elasticity solution for an arbitrary axisymmetric load is presented. Solutions are also provided for a layer on a rigid smooth base which can be considered as a special case of the Winkler foundation.

Solutions to problems involving a layer supported by foundations modeled as a Winkler medium have many applications, particularly in geophysics, and the geotechnical and ice engineering fields (Westergaard, 1926; Hetényi, 1946; Timoshenko and Woinowsky-Krieger, 1959; Selvadurai, 1979; Turcotte, 1979; Ashton, 1986). A general treatment of a layer supported by another layer or a half space was first presented by Burmister (1945). Rather surprisingly there has apparently been no such treatment provided for a layer supported by a Winkler foundation other than the study by Nevel (1970) for a uniformly distributed load over a circular area. However, a survey of the literature revealed that there have been a considerable number of studies involving plates on Winkler foundations. From the comparisons made in this paper between plate solutions and layer solutions, thin plate theory can be used only if the ratio of the characteristic length to the layer depth is large enough. Furthermore, plate theories do not readily furnish an accurate representation of the associated contact pressure distributions, the indentation and applied load versus extent of contact, and the local stresses and moments in most cases.

The limitations of the Winkler foundation model have long been known, particularly in the context of geotechnical engineering (Terzaghi, 1955). Horvath (1989) recently traced the historical development of improvements to Winkler's model. In spite of the uncertainties associated with Winkler's subgrade model, American foundation engineering practice with regard to subgrade models used in routine design practice has changed very little over the last four decades. However, in geophysics (e.g. crustal flexure, Turcotte, 1979) and in ice engineering (Ashton, 1986) the Winkler model is used with far less uncertainty. In fact, the bearing capacity of ice sheets is characterized in terms of the characteristic length, with the Winkler modulus being given by the specific weight of water; the current method to determine the modulus of elasticity of a floating ice sheet is to determine the characteristic length (Sodhi *et al.*, 1982).

Using the fundamental elasticity solution for an arbitrary surface load presented in the Appendix, the title problems are reduced to the solution of a single integral equation. This integral equation is formulated in terms of a rather arbitrary indenter profile. The primary physical equations sought are the contact pressure distributions, contact radii, moments and indentations. Comparisons are made with the asymptotic half space and rigid base solutions, including very thin layer approximations in the latter case. As an approximation of a softer foundation or relatively shallow layer, thin plate solutions are also derived. These solutions are themselves useful in providing directly the most suitable normalized variables as well as a clear indication of the overall necessity of the full-field elasticity solutions provided in this paper.

All three indentation problems belong to a class characterized by Dundurs (1975) as advancing contact, for which the loaded contact regions are not contained within the initial contact regions. An important feature of advancing contact is that the relations among load, contact radius, displacements and stresses are nonlinear. This can be verified from the results throughout this paper. The results presented do not vary with Poisson's ratio except the bending moment and stresses, in which case $\nu = 0.3$ is used.

FORMULATION

The axisymmetric problem of an infinite layer supported by a Winkler foundation and axisymmetrically loaded on the upper surface by a pressure $p(r)$ can be described as follows (Fig. 1a)

$$\sigma_z(r,0) = -p(r), \qquad \tau_{rz}(r,0) = 0, \tag{1a,b}$$

$$\sigma_z(r,h) = -kw(r,h), \quad \tau_{rz}(r,h) = 0, \tag{1c,d}$$

where k is the stiffness of the Winkler foundation and h is the depth of the layer. The full-field elasticity solution of this problem is derived and presented in the Appendix.

For a rigid indenter on a layer, the boundary conditions on the upper surface are

$$w(r,0) = \delta - f(r), \quad p(r) > 0, \quad \text{for} \quad r < c; \quad p(r) = 0, \quad \text{for} \quad r > c \tag{2a,b,c}$$

where δ is displacement at the center of the indenter, c is the contact radius and $f(r)$ is the

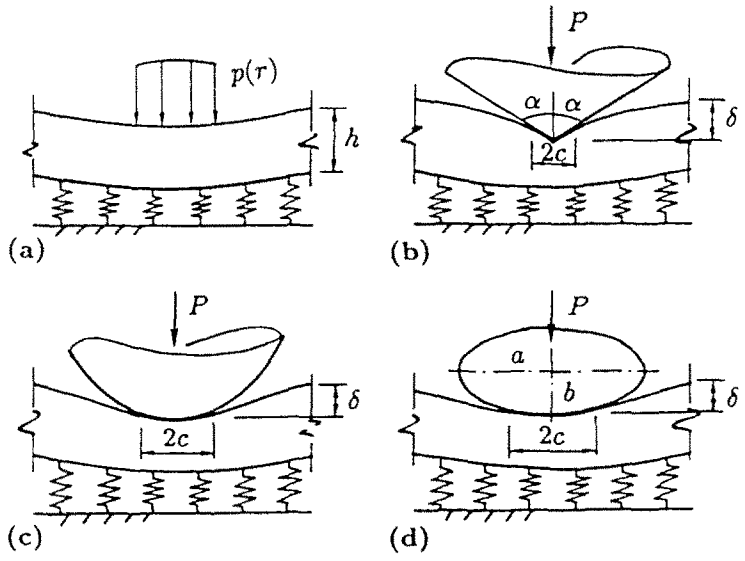

Fig. 1. Problem configurations: (a) an axisymmetric load on a layer, (b) a conical indenter on the layer, (c) a paraboloidal indenter on the layer, (d) an ellipsoidal indenter on the layer.

surface profile of the indenter. For the conical, paraboloidal and ellipsoidal indenters (Figs 1b,c,d), $f(r)$ can be expressed, respectively, as

$$f(r) = r\cot\alpha, \tag{3a}$$

$$f(r) = r^2/2\rho, \tag{3b}$$

$$f(r) = e(a-\sqrt{a^2-r^2}), \tag{3c}$$

where ρ is the radius of curvature and $e = b/a$.

The parameter l/h is a useful measure of the interaction between the layer and the underlying foundation; l is usually called the "characteristic length" or the "radius of relative stiffness" (Westergaard, 1926) and is defined by

$$l^4 = D/k, \quad D = E'h^3/12, \tag{4a,b}$$

in which D is the flexural rigidity of the layer and $E' = E/(1-\nu^2)$; E and ν are the elasticity modulus and Poisson's ratio of the layer, respectively. Clearly, when the Winkler foundation is infinitely rigid, $l = 0$, and the elasticity solutions (A3)–(A8) reduce to the fundamental solutions for a layer on a rigid base (Burmister, 1945). To ascertain the general variation of l/h, a few typical ranges are presented in Table 1, in which l/h is given by (4a,b). However, in practical terms it should be pointed out that the Winkler foundation model is a convenient approximation and that the stiffness parameter k is generally not well defined (except in the case of a floating ice sheet). The value of k depends on the load distribution and intensity and also on the depth of the underlying material.

As shown in the Appendix, if the nonzero portion of the surface pressure is expressed as

$$p(r) = -\sigma_z(r,0) = -\int_r^c \frac{\phi(t)\,\mathrm{d}t}{\sqrt{t^2-r^2}}, \quad (0 \leqslant r \leqslant c) \tag{5}$$

the auxiliary function $\phi(t)$ must satisfy the equation

$$\phi(t) = \frac{2}{\pi}\int_0^c \phi(s)K(t,s)\,\mathrm{d}s - g(t), \quad 0 \leqslant t \leqslant c \tag{6}$$

where, with $L^*(\xi h)$ defined in (A16)

$$K(t,s) = \int_0^\infty L^*(\xi h)\sin(\xi t)\sin(\xi s)\,\mathrm{d}\xi, \tag{7a}$$

$$g(t) = \frac{E'}{\pi t}\frac{\mathrm{d}}{\mathrm{d}t}\int_0^t \frac{r^2 f'(r)}{\sqrt{t^2-r^2}}\,\mathrm{d}r. \tag{7b}$$

Since $\phi(t)$ is a regular function for the indenter profiles considered, this is a Fredholm

Table 1. Typical range of l/h for different material combinations

	E' (GPa)	k (MN m^{-3})	h (m)	l/h
Lithosphere/mantle	20–100	0.025–0.035	10^5–2×10^5	0.7–1.4
Steel/concrete	207	5000–20000	0.02–0.1	1.7–3.6
Concrete/soil	20–30	50–220	0.1–1	1.7–4.6
Freshwater ice/water	3–7	0.01	0.05–1	12–33
Steel/rubber	207	0.03–0.1	0.02–0.1	36–73

integral equation of the second kind and is solved numerically using Gauss–Legendre quadrature.

Once the function $\phi(t)$ has been determined, all other physical quantities can be calculated from $\phi(t)$; from (5) and the equilibrium condition, the total load is

$$P = 2\pi \int_0^c p(r) r \, dr = -2\pi \int_0^c t\phi(t) \, dt, \tag{8}$$

and the center displacement from (A11) is

$$\delta = -\left\{ \int_0^c \phi(t) \, dt + \frac{2}{\pi} \int_0^c \phi(t) \int_0^c L^*(\xi h) \frac{\sin(\xi t)}{\xi} \, d\xi \, dt \right\} \Big/ E'. \tag{9}$$

In a similar way, the normal stress and the bending moment at the center can also be calculated.

Based on thin plate theory, the bending moment $M(r)$ and the stress $\sigma_r(r, h)$ are proportional, with $\sigma(r) = 6M(r)/h^2$. It has been found that this equation tends to overestimate the stress at the lower surface of thicker layers, approximately 20% for $l/h = 1$, and 5% for $l/h = 2$. However, for thinner layers with $l/h \geq 4$, the differences are minimal and the stress can be calculated directly from the moment.

The behavior of the kernel function $K(t, s)$ defined in (7a) depends on the function $L^*(\xi h)$ [see (A16)] which in turn depends on the values of l/h and decays exponentially as the argument becomes large. When $l/h > 4$ (that is, a softer foundation or shallow layer), the area enclosed by $L^*(\xi h)$ and the horizontal axis is concentrated near the origin. The integration then needs to be evaluated only over a small range of ξ. Therefore, Gauss quadrature can be used for these cases. On the other hand, when $l/h < 4$, the area spreads over a wider range, and evaluating the integral using Gauss quadrature tends to be time consuming. A better procedure in this case is to express the function $L^*(\xi h)$ in the form of an exponential series such that the integration can be done analytically. This method is discussed by Dempsey *et al.* (1989).

The function $g(t)$ in (7b) can be calculated for different indenter profiles. For the conical, paraboloidal and ellipsoidal indenter, respectively,

$$g(t) = E' \cot \alpha/2, \tag{10a}$$

$$g(t) = 2tE'/\pi\rho, \tag{10b}$$

$$g(t) = eE' \left\{ \tanh^{-1}\left(\frac{t}{a}\right) + \frac{t/a}{1-(t/a)^2} \right\} \Big/ \pi. \tag{10c}$$

When the ratio of the contact radius to the semiaxis c/a is small, (10c) can be approximated by the expression in (10b) with $1/\rho$ replaced by the length e/a. For a spherical indenter ($e = 1$), the latter expression is equivalent to that in (10b). Therefore, an ellipsoidal indenter can be treated as a paraboloidal indenter if the ratio c/a is small ($c/a < 0.1$). Such a simplification is made not only for mathematical convenience, but also because the fundamental assumption of small deformations in linear elasticity requires that the ratio c/a be small. For an ellipsoidal indenter with a small e value, however, a meaningful solution for a large c/a value is possible and the expression (10c) then has to be used. A rigid ellipsoidal indenter becomes a rigid flat-ended cylindrical indenter as $e \to 0$. The flat-ended cylindrical indenter is treated in this paper by allowing $e \to 0$.

More general solutions are readily obtained by expressing the indenter profile in polynomial form as

$$f(r) = \sum_{n=1}^{\infty} a_n r^n. \tag{11}$$

An analytical polynomial expression for $g(t)$ can then be obtained. The associated solution can be carried out exactly as the other cases so long as the indenter has no sharp edge in contact with the layer.

HALF SPACE SOLUTIONS

When the layer depth becomes infinitely large in comparison to the contact region, the title problem reduces to the indentation of an elastic half space by rigid punches. Analytical solutions can be derived to provide checking cases. As $c/h \to 0$, $L^*(\xi h) \to 0$ and $K(t, s) \to 0$, then (6) and (9) become

$$\phi(t) = -g(t), \quad \delta = -\left\{\int_0^c \phi(t)\,\mathrm{d}t\right\}\Big/ E'. \tag{12a,b}$$

The contact pressure and load can be calculated from (5) and (8), respectively.

It is important to note, from (12a), that function $\phi(t)$ is a regular function for the three indenter profiles discussed. For a finite layer depth, the shape of $\phi(t)$ may be different, but there will be no singularity involved. Thus Gauss–Legendre quadrature can be used to solve for $\phi(t)$ from (6). The formulation given above quickly provides the following results, most of which have long been known (Timoshenko and Goodier, 1969).

For a conical indenter (Sneddon, 1951)

$$\frac{\delta \tan\alpha}{c} = \frac{\pi}{2}, \quad \frac{P \tan\alpha}{E' c^2} = \frac{\pi}{2}, \quad \frac{p(r)}{p_{av}} = \cosh^{-1}\left(\frac{c}{r}\right). \tag{13a,b,c}$$

For a paraboloidal indenter (Hertz, 1881)

$$\frac{\delta\rho}{c^2} = 1, \quad \frac{P\rho}{E' c^3} = \frac{4}{3}, \quad \frac{p(r)}{p_{av}} = \tfrac{3}{2}\sqrt{1-(r/c)^2}. \tag{14a,b,c}$$

For an ellipsoidal indenter (Segedin, 1957),

$$\frac{\delta}{ec} = \tanh^{-1}\left(\frac{c}{a}\right), \quad \frac{P}{E' c^2 e} = \left(\frac{a}{c}\right)^2 \left\{\left[\left(\frac{c}{a}\right)^2 + 1\right]\tanh^{-1}\left(\frac{c}{a}\right) - \frac{c}{a}\right\}, \tag{15a,b}$$

$$\frac{p(r)}{E' e} = \frac{1}{\pi}\int_r^c \left\{\tanh^{-1}\left(\frac{t}{a}\right) + \frac{t/a}{1-(t/a)^2}\right\}\frac{\mathrm{d}t}{\sqrt{t^2 - r^2}}. \tag{15c}$$

The last expression can be evaluated numerically.

Finally, the case of an ellipsoidal indenter with $e \to 0$ can be treated as a flat-ended cylindrical indenter, for which equations were derived by Boussinesq (1885), with further work being done by Sneddon (1946),

$$\frac{2\delta a E'}{P} = 1, \quad \frac{p(r)}{p_{av}} = \frac{1}{2\sqrt{1-(r/a)^2}}. \tag{16a,b}$$

For an ellipsoidal indenter on a half space, the contact pressure distributions are

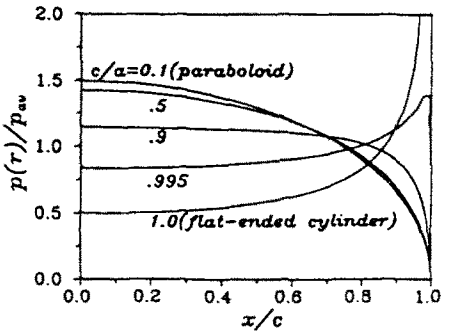

Fig. 2. Contact pressure distributions of an ellipsoidal indenter on a half space.

plotted in Fig. 2 for different c/a ratios. The distribution patterns gradually change from that of a paraboloidal indenter to that of a flat-ended cylinder as c/a increases.

RIGID BASE SOLUTIONS

Another interesting special case for the title problem is an elastic layer supported by a rigid smooth base. The associated solution is obtained by letting the stiffness of the Winkler foundation approach infinity ($l/h \to 0$). For a conical indenter, the total load and center displacement are plotted in Fig. 3a. The center pressure for the conical indenter is infinite. The center displacement, total load, and the center pressure for an ellipsoidal indenter are plotted in Figs 3b,c,d, respectively. The same quantities for a paraboloidal indenter are very similar to those of $c/a = 0.1$ with a/e in the ordinate being replaced by ρ in Figs 3b,c,d. More detailed discussion for this case can be found in a paper by Li and Dempsey (1990).

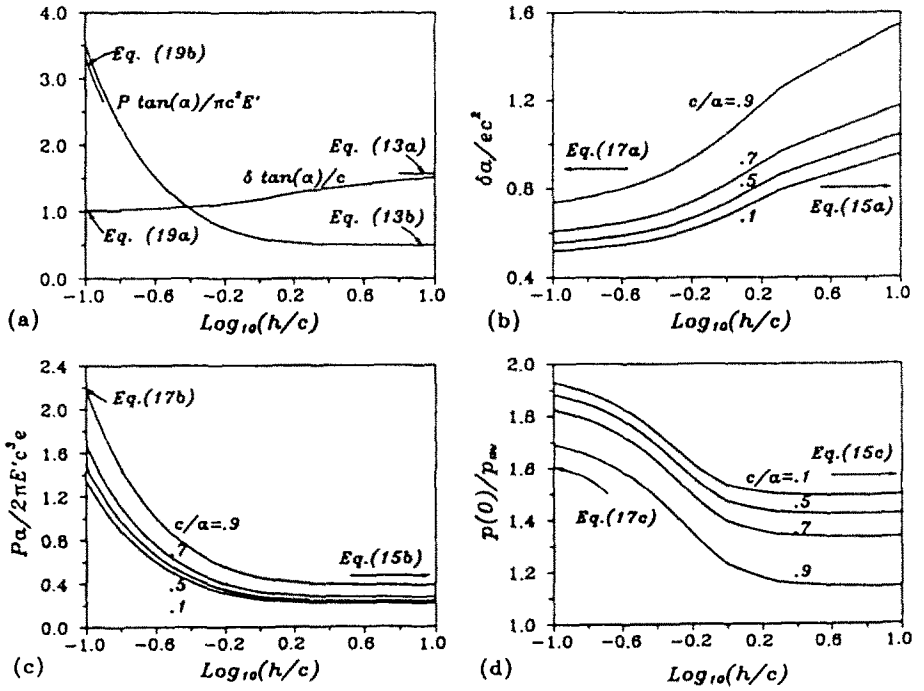

Fig. 3. Indentation of a layer underlain by a rigid smooth base: (a) load and displacement of a conical indenter, (b) displacement of ellipsoidal indenters (EI), (c) load of EI, (d) center pressure of EI. [For a paraboloidal indenter, follow the $c/a = 0.1$ lines in (b), (c), (d) and replace a/e of ordinates in (b), (c) by ρ.]

For a very thin layer, $h/c \to 0$, asymptotic solutions can be derived with two assumptions: (1) the material under the indenter is in a state of confined compression, i.e. $\sigma = \varepsilon E(1-\nu)/(1+\nu)(1-2\nu) \approx \varepsilon E'$, and (2) the layer deformation at the edge of the contact region is zero. For instance, the approximate surface displacement and pressure distribution for an ellipsoidal indenter on a thin layer can be expressed as $w(r) = hp(r)/E' = \delta - e(a - \sqrt{a^2 - r^2})$, where $\delta = e(a - \sqrt{a^2 - c^2})$ since $w(c) = 0$ is assumed. After integration and rearrangement, the following relations can be derived,

$$\frac{\delta a}{ec^2} = \frac{a^2}{c^2}(1 - \sqrt{1-(c/a)^2}), \tag{17a}$$

$$\frac{Pa}{2\pi E' c^3 e} = \frac{c}{h}\left\{\frac{1}{2}\frac{\delta a}{ec^2} - \frac{1}{2}\frac{a^2}{c^2} + \frac{1}{3}\frac{a^4}{c^4}(1-(c/a)^2)^{3/2}\right\}. \tag{17b}$$

$$\frac{p(0)}{p_{av}} = \frac{c}{2h}\frac{\delta a}{ec^2}\frac{2\pi E' c^3 e}{Pa}. \tag{17c}$$

For a paraboloidal indenter on a thin layer, assuming c/a small and replacing a/e by ρ, the approximate expressions are simplified to

$$\frac{\delta\rho}{c^2} = \frac{1}{2}, \quad \frac{P\rho}{2\pi E' c^3} = \frac{1}{8}\frac{c}{h}, \quad \frac{p(0)}{p_{av}} = 2. \tag{18a,b,c}$$

For a conical indenter, similar relations can be found as

$$\frac{\delta \tan\alpha}{c} = 1, \quad \frac{P\tan\alpha}{\pi c^2 E'} = \frac{c}{3h}. \tag{19a,b}$$

CONICAL INDENTER

The relations between the total load, contact radius, center displacement and center bending moment for the conical indenter on a layer underlain by a Winkler foundation are plotted in Fig. 4. Note that the bending moment in Fig. 4d increases as l/h increases. The limiting value for the moment is infinity for $l/h \to \infty$, as predicted by thin plate theory.

Since the layer behaves more like a thin plate as the l/h ratio increases, thin plate solutions serve to provide appropriate normalization in these diagrams. The corresponding solutions are obtained from the point load case, for which the solution was first provided by Hertz (1884) (see also Timoshenko and Woinowsky-Krieger, 1959)

$$w(r) = -\frac{Pl^2}{2\pi D}\,\mathrm{kei}\,(r/l), \quad \delta = w(0) = \frac{Pl^2}{8D}. \tag{20a,b}$$

Equation (20b) produces the straight line in Fig. 4c. It can be seen that the elasticity solution is indeed well approximated by the plate solution as l/h increases. The relationship between indentation and contact radius (Fig. 4a), and the load and contact radius (Fig. 4b) are not well approximated by thin plate theory.

As the total load increases, the conical indenter may start to make contact with the layer surface over a separate annular region in addition to the central contact region. This case should be excluded since the formulation is not valid for multiple regions. From thin plate theory, the condition to avoid the case of multiple contact regions is

$$w(r) < w(0) - r\cot\alpha, \quad \text{or} \quad Pl\tan(\alpha)/D < 11.6. \tag{21a,b}$$

The ranges of total load in Fig. 4 are set according to this condition. The exact value of the critical load for a layer to exhibit contact regions is difficult to derive from the elasticity

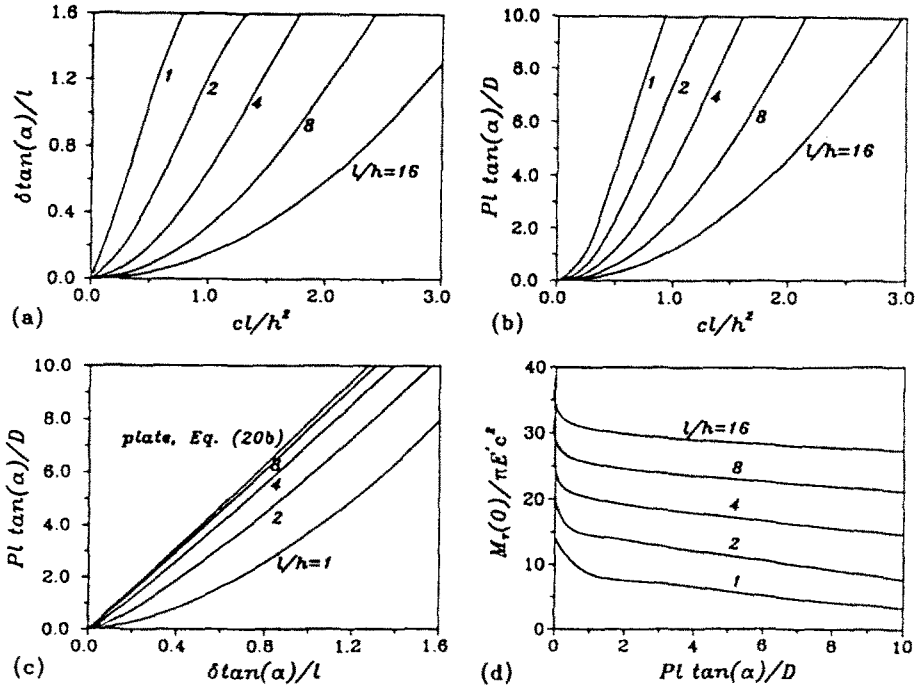

Fig. 4. Conical indenter on a layer underlain by a Winkler foundation: (a) load vs contact radius, (b) center displacement vs contact radius, (c) load vs center displacement, (d) center bending moment vs load.

formulation. However, it can be anticipated that the range for a thicker layer is smaller, since the total deformation of a layer can be considered approximately as the combination of the plate deformation and the local deformation. The larger the local deformation, the easier it is for multiple contact regions to occur.

Within the limitation of (21b), the contact pressure distributions for a conical indenter are essentially the same as given in (13c) for a half space: infinite at the center and zero at the edge. The pressure shifts slightly towards the center as c/l and l/h increase.

PARABOLOIDAL INDENTER

Shown in Fig. 5 are the contact pressure distributions given different c/l and l/h values for a paraboloidal indenter on a layer underlain by a Winkler foundation. As the c/l, l/h ratios increase, the contact pressure distribution gradually changes from a hemispherical Hertzian contact pressure distribution to the large area contact pressure distributions of the type found by Keer and Miller (1983) for a circular layer supported elastically on edge supports. The large concentration of contact pressure at the edge of the contact region approaches the limiting line pressure predicted by plate theory. Clearly, the plate solutions become more accurate as both c/l and l/h increase. Otherwise, elasticity solutions have to be used. Shown in Fig. 6 are the associated relations of displacement, load, contact radius and center bending moment. Note that variables are normalized so that the elasticity solutions and the plate solutions can be plotted together. Again, the plate solution becomes more accurate as c/l and l/h increase. Surprisingly good agreement is found in Fig. 6c for the load displacement relation. The advantage of the plate solution, of course, is that all the relations can be expressed analytically. The derivation of the latter solution is now described briefly.

The surface displacement of an infinitely large thin plate on a Winkler foundation outside the contact region can be expressed as (Timoshenko and Woinowsky-Krieger, 1959)

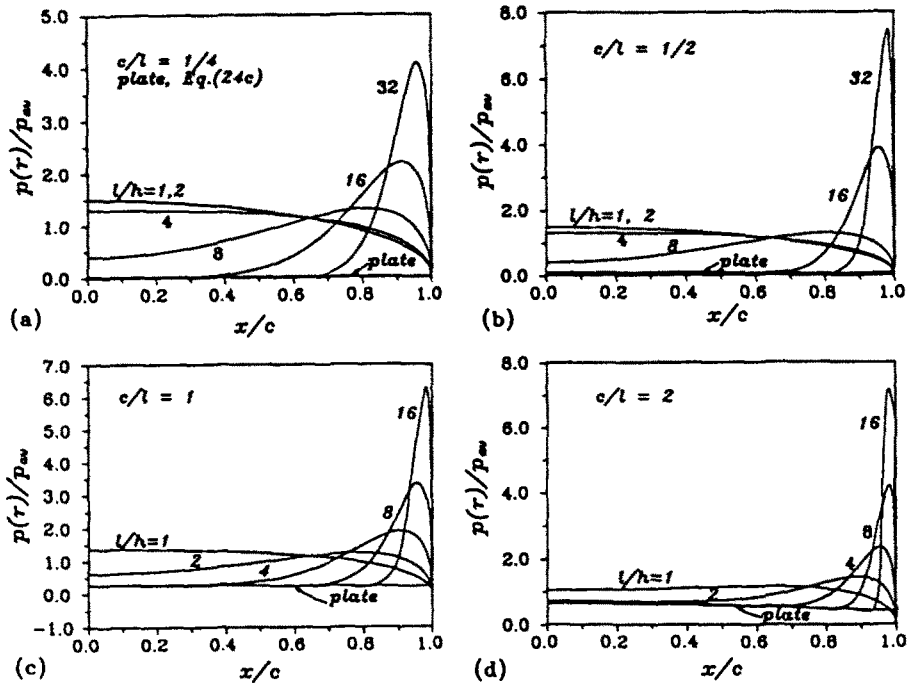

Fig. 5. Contact pressure for a paraboloidal indenter on a layer underlain by a Winkler foundation.

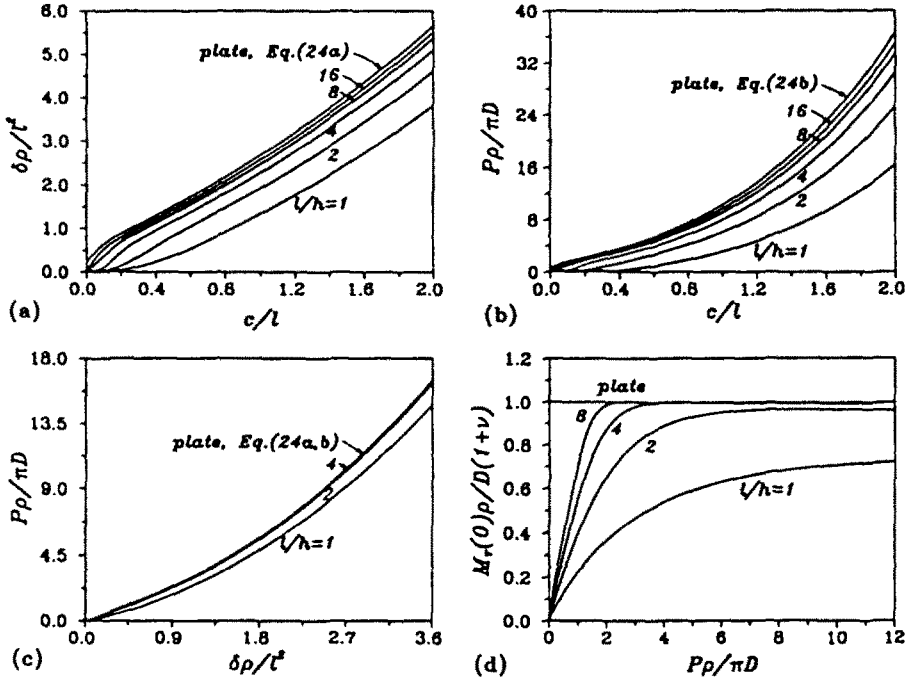

Fig. 6. Paraboloidal indenter on a layer underlain by a Winkler foundation : (a) center displacement vs contact radius, (b) load vs contact radius, (c) load vs center displacement, (d) center bending moment vs load.

$$w_p(r) = C_1 \ker(r/l) + C_2 \operatorname{kei}(r/l). \tag{22}$$

The two constants can be determined from the compatibility conditions at the edge of the contact region, i.e.

$$w'_p(c) = -c/\rho, \quad w''_p(c) = -1/\rho. \tag{23a,b}$$

Within the contact region, the curvature of the plate is constant. It can be concluded, therefore, that the bending moments are constant, that the shear forces are zero, and that the contact pressure is the same as the support reaction which is proportional to the displacement for a Winkler foundation. The shear force exerted by the external part of the plate is balanced by a circular line force on the indenter. The displacement of the indenter can be calculated from the displacement at the edge of the contact region and the total load is the summation of the distributed pressure and the line force. The final relationships derived are now expressed as functions of c/l:

$$\frac{\delta\rho}{l^2} = \frac{c^2}{2l^2} + \frac{2(AB' - A'B) - (c/l)(A^2 + B^2)}{A'A + B'B}, \tag{24a}$$

$$\frac{P\rho}{\pi D} = \frac{c^4}{4l^4} + \frac{4(c/l)^2(AB' - A'B) - 4(c/l)(A'^2 + B'^2) - (c/l)^3(A^2 + B^2)}{A'A + B'B}, \tag{24b}$$

$$\frac{p(r)}{p_{av}} = \frac{\pi D}{P\rho}\left\{\frac{\delta\rho}{l^2} - \frac{1}{2}\frac{r^2}{l^2}\right\}\left(\frac{c}{l}\right)^2, \tag{24c}$$

where

$$A = \mathrm{ker}\,(c/l), \quad B = \mathrm{kei}\,(c/l), \quad A' = \mathrm{ker}'\,(c/l), \quad B' = \mathrm{kei}'\,(c/l), \tag{25}$$

are the Kelvin functions of the first kind and their derivatives. For a layer with a large l/h value, the transverse and shear deformation can be neglected and the above expressions provide a simplified solution.

ELLIPSOIDAL INDENTER

Contact pressure distributions for an ellipsoidal indenter on a layer underlain by a Winkler foundation are shown in Fig. 7 for different c/a, l/h and c/h ratios. Though different

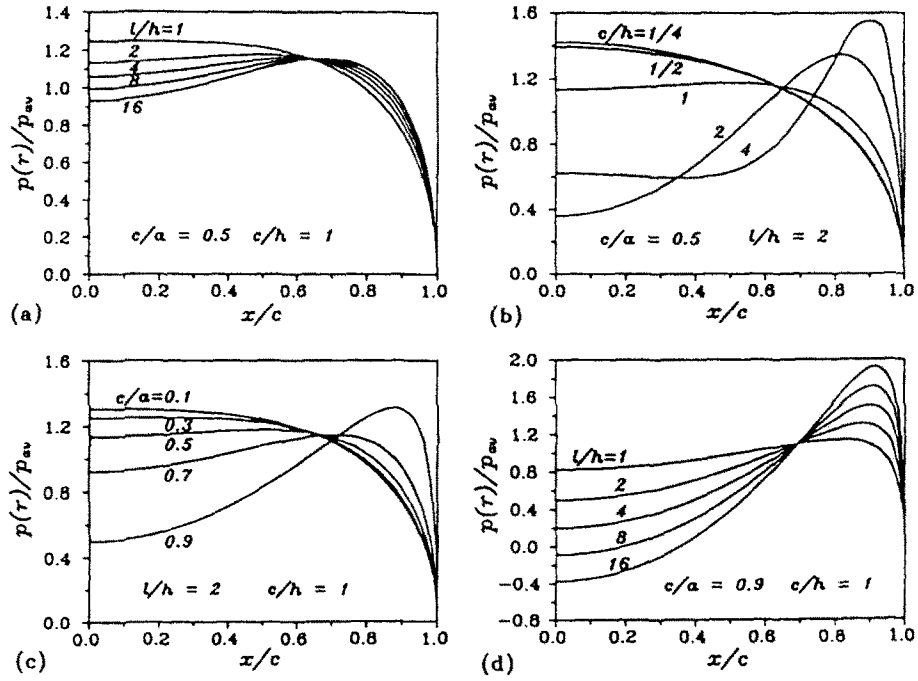

Fig. 7. Contact pressure for an ellipsoidal indenter on a layer underlain by a Winkler foundation.

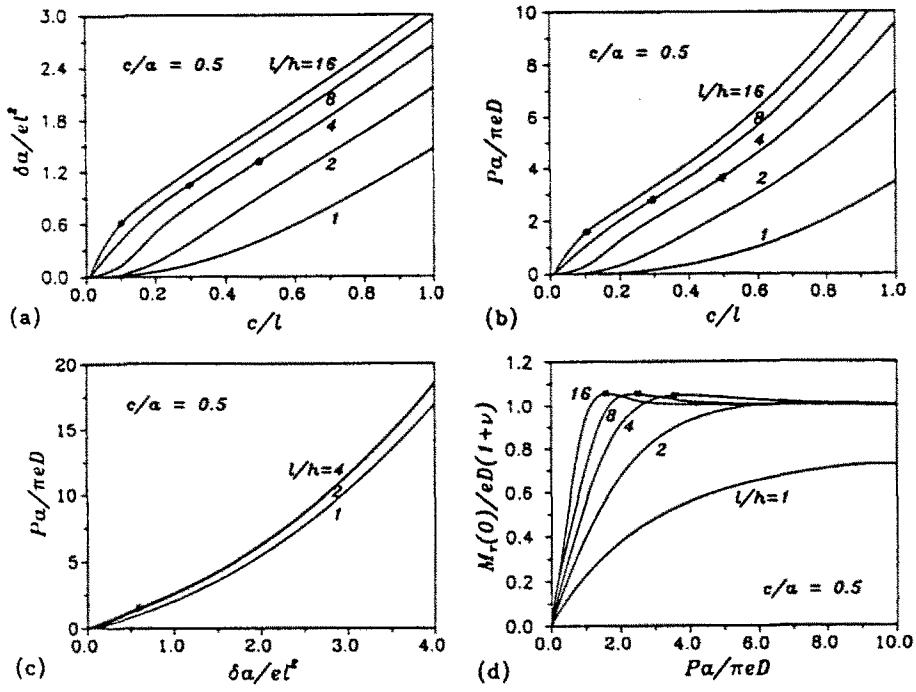

Fig. 8. Ellipsoidal indenter on a layer underlain by a Winkler foundation $c/a = 0.5$: (a) center displacement vs contact radius, (b) load vs contact radius, (c) load vs center displacement, (d) center bending moment vs load.

choices of parameters produce different curves, these figures illustrate the general tendency: the maximum contact pressure shifts from the center toward the edge of the contact region as the values of c/a, l/h and c/h increase. At some juncture, however, the contact pressure becomes negative within the contact region (Fig. 7d). The solution then becomes invalid unless the indenter is assumed to be bonded to the layer surface.

In comparison to the paraboloidal indenter, there is one more controlling parameter c/a involved, which means the size of the indenter is also important. This makes a complete presentation of results difficult. The relations between the displacement, load, contact radius and center bending moment are plotted for $c/a = 0.5$ in Fig. 8 and for $c/a = 0.9$ in Fig. 9, respectively. For $c/a \leqslant 0.1$, the diagrams are the same as for the paraboloidal indenter case with ρ being replaced by a/e. It has been found that negative contact pressure is more likely to occur as c/a increases. Therefore, the geometry most likely to exhibit contact separation is a flat-ended cylinder since then $c/a = 1$. The occurrence of negative pressure is indicated by the asterisks on the line in the diagrams. Beyond these asterisks, the indenter has to be assumed bonded to the layer surface for the results to be applicable.

It is important to note, from (10c) for the ellipsoidal indenter, that the function $g(t)$ is proportional to the eccentricity of the ellipsoidal indenter e. Consequently, the total load, the displacement, and stresses and bending moments are all proportional to e. Further, the ratios of load to displacement, and stress to total load, are independent of e for the same reason. Presentation of the results can, therefore, be simplified significantly. To this end, it is interesting to note the conclusion, reached by Segedin (1957) for an ellipsoidal indenter on a half space, that the load–displacement ratio is the same as that of a flat-ended indenter if $c = a$.

CONCLUSIONS

Three different axisymmetric indenter profiles have been considered: conical, paraboloidal and ellipsoidal. The contact behaviors do not depend on the size of indenters for the first two indenters, but do depend on the size of the last indenter. This makes the

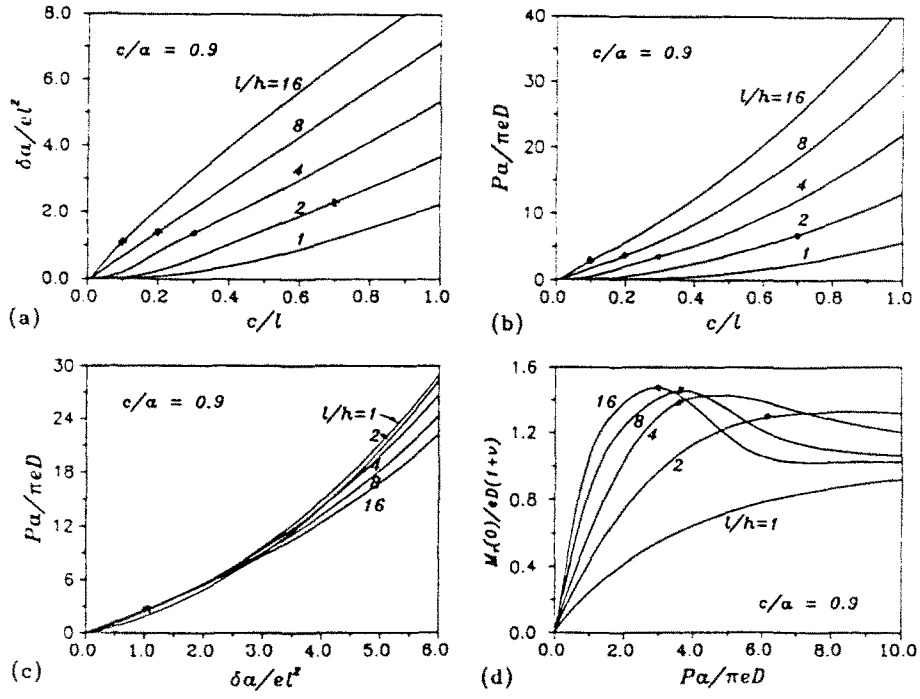

Fig. 9. Ellipsoidal indenter on a layer underlain by a Winkler foundation $c/a = 0.9$: (a) center displacement vs contact radius, (b) load vs contact radius, (c) load vs center displacement, (d) center bending moment vs load.

complete presentation of results difficult for the ellipsoidal indenter. Interestingly, the load–displacement ratio and stress–load ratio do not depend on e, the eccentricity of the ellipsoid.

The most important parameter in the title problem is the ratio of characteristic length to the layer depth, l/h. The greater the l/h ratio, the softer the foundation, or the thinner the layer. Solutions for an elastic half space and a layer on a rigid smooth base are derived as special cases by letting $l/h \to 0$. On the other hand, as the layer depth reduces and the l/h ratio increases, the transverse deformation and the shear deformation of the layer become less significant, in which case, approximate solutions derived from the thin plate theory are somewhat applicable. These solutions include the load–displacement relation for the conical indenter, the relations among load, contact radius, maximum bending moment and displacement for the paraboloidal indenter. The load versus displacement response for the paraboloidal indenter is very accurate if $l/h \geqslant 4$, while other expressions provide limiting values as $l/h \to \infty$. The derivation of thin plate solutions for the ellipsoidal indenter is more complicated and the final expressions do not serve well as "simplified solutions".

Hertzian contact pressure distributions are observed for both paraboloidal and ellipsoidal indenters when the contact radii are small. The distributions gradually change to those of large area contact, with the maximum pressure shifting from the center to the edge of the contact region, as the ratios of c/l, l/h and c/a increase. Separation between the ellipsoidal indenter and the layer surface is more likely to occur for larger c/l, l/h and c/a ratios. Then a different formulation is required unless the indenter is assumed to be bonded to the layer surface.

Acknowledgement—This work has been supported in part by the U.S. Army under contract no. DACA 89-88-K-0013.

REFERENCES

Ashton, G. D. (1986). *River and Lake Ice Engineering*. Water Resources Publications, Colorado.

Boussinesq, J. (1885). *Application des Potentials à l'Etude l'Equilibre et du Mouvement des Solides Elastiques*. Gauthier-Villars, Paris.

Burmister, D. M. (1945). The general theory of stress and displacements in layered soil system, II. *J. Appl. Phys.* **16**, 126–127.
Dempsey, J. P., Zhao, Z. G., Minnetyan, L. and Li, H. (1989). Plane contact of an elastic layer supported by a Winkler foundation. *ASME J. Appl. Mech.* (in press).
Dundurs, J. (1975). Properties of elastic bodies in contact. In *The Mechanics of the Contact between Deformable Bodies* (Edited by A. D. De Pater and J. J. Kalker). Delft University Press, Delft.
Hertz, H. (1881). On the contact of elastic solids. *J. reine angew. Math.* **92**, 156–171. English translation in Jones, D. E. and Schott, G. A. (1896). *Miscellaneous Papers*. Macmillan, London.
Hertz, H. (1884). On the equilibrium of floating elastic plate. *Wiedemann's Annalen* **22**, 449–455. English translation in Jones, D. E. and Schott, G. A., (1896). *Miscellaneous Papers*. Macmillan, London.
Hetényi, M. (1946). *Beams on Elastic Foundation*. The University of Michigan Press, Ann Arbor.
Horvath, J. S. (1989). Subgrade models for soil–structure interaction analysis. In *Foundation engineering* (Edited by Fred H. Kulhawy), Vol. 1, pp. 599–612.
Keer, L. M. and Miller, G. R. (1983). Contact between an elastically supported circular plate and rigid indenter. *Int. J. Engng Sci.* **21**, 681–690.
Li, H. and Dempsey, J. P. (1989). Axisymmetric contact of an elastic layer underlain by a rigid base. *Int. J. Numer. Meth. Engng* **29**, 57–72 (1990).
Nevel, D. E. (1970). Concentrated loads of plates. Unpublished Report, U.S. Army Cold Regions Research and Engineering Laboratory, Hanover, New Hampshire.
Popov, G. Ia. (1962). The contact problem of the theory of elasticity for the case of a circular area of contact. *PMM J. Appl. Math Mech.* **26**, 207–225.
Segedin, C. M. (1957). The relation between load and penetration for a spherical punch. *Mathematika* **4**, 156–161.
Selvadurai, A. P. S. (1979). *Elastic Analysis of Soil–Foundation Interaction*. Elsevier/North-Holland, New York.
Sneddon, I. N. (1946). Boussinesq's problem for a flat-ended cylinder. *Proc. Camb. Phil. Soc.* **42**, 29–39.
Sneddon, I. N. (1951). *Fourier Transforms*. McGraw-Hill, New York.
Sneddon, I. N. (1960). The elementary solution of dual integral equations. *Proc. Glasg. Math. Assoc.* **4**, 106–114.
Sodhi, D. S., Kato, K., Haynes, F. D. and Hirayama, K. (1982). Determining the characteristic length of model ice sheets. *Cold Regions Sci. Technol.* **6**, 99–104.
Terzaghi, K. (1955). Evaluation of coefficients of subgrade reaction. *Geotechnique* **5**, 297–326.
Timoshenko, S. and Goodier, J. N. (1969). *Theory of Elasticity*, 3rd edn. McGraw-Hill, New York.
Timoshenko, S. and Woinowsky-Krieger (1959). *Theory of Plates and Shells*, 2nd edn. McGraw-Hill, New York.
Turcotte, D. L. (1979). Flexure. *Adv. Geophys.* **21**, 51–86.
Westergaard, H. M. (1926). Stress in concrete pavements computed by theoretical analysis. *Publ. Rds* **7**, 25–35.

APPENDIX: GENERAL AXISYMMETRIC SOLUTION

The axisymmetric problem of an infinite layer supported by a Winkler foundation and axisymmetrically loaded on the upper surface is solved by finding a stress function $\phi(r, z)$, which satisfies the biharmonic equation

$$\nabla^4\phi(r,z) = 0, \tag{A1}$$

as well as the boundary conditions in (1a–d). The solution of this equation for the problem can be expressed as

$$\phi(r,z) = \int_0^\infty \xi\{[C_1(\xi)+C_3(\xi)z]\cosh(\xi z)+[C_2(\xi)+C_4(\xi)z]\sinh(\xi z)\}J_0(r\xi)\,\mathrm{d}\xi. \tag{A2}$$

The functions $C_1(\xi)$, $C_2(\xi)$, $C_3(\xi)$ and $C_4(\xi)$ are determined by the boundary conditions (1a–d). The stresses and displacements are then calculated from $\phi(r, z)$ (Sneddon, 1951). The final expressions are found to be, with $S = \sinh\beta$, $C = \cosh\beta$, $S_z = \sinh\xi z$, $C_z = \cosh\xi z$ and $\beta = \xi h$.

$$\sigma_r(r,z) = \int_0^\infty \frac{\xi F(\xi)}{d(\beta)}\left\{[\xi zS^2-(\beta+SC)]S_z+[S^2+\beta^2-\xi z(\beta+SC)]C_z+\frac{h^4}{6\beta l^4}\{[\xi zSC-S^2]S_z\right.$$
$$\left.+[SC-\beta-\xi zS^2]C_z\}\right\}J_0(\xi r)\,\mathrm{d}\xi-\frac{1}{r}\int_0^\infty\frac{F(\xi)}{d(\beta)}\left\{[\xi zS^2-(1-2\nu)(\beta+SC)]S_z+[(1-2\nu)S^2\right.$$
$$\left.+\beta^2-\xi z(\beta+SC)]C_z+\frac{h^4}{6\beta l^4}\{[\xi zSC-(1-2\nu)S^2]S_z+[(1-2\nu)SC-\beta-\xi zS^2]C_z\}\right\}J_1(\xi r)\,\mathrm{d}\xi, \tag{A3}$$

$$\sigma_\theta(r,z) = 2\nu\int_0^\infty\frac{\xi F(\xi)}{d(\beta)}\left\{S^2C_z-(\beta+SC)S_z+\frac{h^4}{6\beta l^4}\{-S^2S_z+SCC_z\}\right\}J_0(\xi r)\,\mathrm{d}\xi$$
$$+\frac{1}{r}\int_0^\infty\frac{F(\xi)}{d(\beta)}\left\{[\xi zS^2-(1-2\nu)(\beta+SC)]S_z+[(1-2\nu)S^2+\beta^2-\xi z(\beta+SC)]C_z+\frac{h^4}{6\beta l^4}\{[\xi zSC-(1-2\nu)S^2]S_z\right.$$
$$\left.+[(1-2\nu)SC-\beta-\xi zS^2]C_z\}\right\}J_1(\xi r)\,\mathrm{d}\xi. \tag{A4}$$

$$\sigma_z(r,z) = \int_0^\infty \frac{\xi F(\xi)}{d(\beta)} \left\{ -[\xi z S^2 + (\beta + SC)]S_z + [S^2 - \beta^2 + \xi z(\beta + SC)]C_z \right.$$
$$\left. + \frac{h^4}{6\beta l^4}\{-[\xi z SC + S^2]S_z + [SC + \beta + \xi z S^2]C_z\} \right\} J_0(\xi r)\, d\xi, \quad \text{(A5)}$$

$$\sigma_{rz}(r,z) = \int_0^\infty \frac{\xi F(\xi)}{d(\beta)} \left\{ [\beta^2 - \xi z(\beta + SC)]S_z + \xi z S^2 C_z - \frac{h^4}{6\beta l^4}\{[\beta + \xi z S^2]S_z - \xi z SC C_z\} \right\} J_1(\xi r)\, d\xi, \quad \text{(A6)}$$

$$u(r,z) = \frac{1}{2\mu}\int_0^\infty \frac{F(\xi)}{d(\beta)} \left\{ [\xi z S^2 - (1-2\nu)(\beta + SC)]S_z - [\xi z(\beta + SC) - (1-2\nu)S^2 - \beta^2]C_z \right.$$
$$\left. + \frac{h^4}{6\beta l^4}\{[\xi z SC - (1-2\nu)S^2]S_z - [\xi z S^2 + \beta - (1-2\nu)SC]C_z\} \right\} J_1(\xi r)\, d\xi. \quad \text{(A7)}$$

$$w(r,z) = \frac{1}{2\mu}\int_0^\infty \frac{F(\xi)}{d(\beta)} \left\{ [2(1-\nu)S^2 - \beta^2 + \xi z(\beta + SC)]S_z - [2(1-\nu)(\beta + SC) + \xi z S^2]C_z \right.$$
$$\left. + \frac{h^4}{6\beta l^4}\{[2(1-\nu)SC + \beta + \xi z S^2]S_z - [2(1-\nu)S^2 + \xi z SC]C_z\} \right\} J_0(\xi r)\, d\xi, \quad \text{(A8)}$$

where $\beta = \xi h$, $\mu = E/2(1+\nu)$ is the shear modulus, while $F(\xi)$ and $d(\beta)$ are defined as follows

$$F(\xi) = -\int_0^\infty p(r) r J_0(\xi r)\, dr, \quad \text{(A9)}$$

$$d(\beta) = \sinh^2\beta - \beta^2 + \frac{h^4}{6\beta l^4}(\beta + \sinh\beta\cosh\beta). \quad \text{(A10)}$$

The parameter l is defined in (4). Note that the surface displacement can be determined from (A8) simply as

$$w(r,0) = -\frac{2}{E'}\int_0^\infty F(\xi) L(\beta) J_0(\xi r)\, d\xi, \quad \text{(A11)}$$

where $E' = E/(1-\nu^2)$ and

$$L(\beta) = \frac{1}{d(\beta)}\left(\beta + \sinh\beta\cosh\beta + \frac{h^4}{6\beta l^4}\sinh^2\beta\right). \quad \text{(A12)}$$

If the auxiliary function $\phi(t)$ introduced by Sneddon (1960),

$$\xi F(\xi) = \int_0^\infty \phi(t)\sin(\xi t)\, dt, \quad \text{(A13)}$$

is substituted into the surface pressure given by (A5), then

$$p(r) = -\sigma_z(r,0) = -\int_0^\infty \xi F(\xi) J_0(\xi r)\, d\xi = -\int_r^\infty \frac{\phi(t)\, dt}{\sqrt{t^2 - r^2}}. \quad \text{(A14)}$$

Clearly, condition (2c) is automatically satisfied by this substitution. Substituting (A13) into (A11), then into (2a), and differentiating the resulting equation with respect to r give

$$\frac{2}{E'}\int_0^\infty \phi(t)\int_0^\infty L(\beta)\sin(\xi t) J_1(\xi r)\, d\xi\, dt = -f'(r). \quad \text{(A15)}$$

By redefining

$$L(\beta) = 1 + L^*(\beta), \quad \text{(A16)}$$

and noting that

$$\int_0^\infty \sin(\xi t) J_1(\xi r)\, d\xi = \begin{cases} t/r\sqrt{r^2 - t^2}, & t < r \\ 0, & t > r \end{cases} \quad \text{(A17)}$$

it is immediate that eqn (A15) may be written in the form of an Abel integral equation

$$\int_0^r \frac{t\phi(t)}{\sqrt{r^2-t^2}}\,dt = r\int_0^c \phi(t)\hat{K}(r,t)\,dt - \frac{E'}{2}rf'(r), \tag{A18}$$

where

$$\hat{K}(r,t) = \int_0^\infty L^*(\beta)\sin(\xi t)J_1(\xi r)\,d\xi. \tag{A19}$$

The solution of (A18) is (Sneddon, 1960)

$$t\phi(t) = \frac{2}{\pi}\frac{d}{dt}\int_0^t \left\{r\int_0^c \phi(s)\hat{K}(r,s)\,ds - \frac{E'}{2}rf'(r)\right\}\frac{r}{\sqrt{t^2-r^2}}\,dr. \tag{A20}$$

By using the relation

$$\frac{1}{t}\frac{d}{dt}\int_0^t \frac{r^2J_1(\xi r)}{\sqrt{t^2-r^2}}\,dr = \sin(\xi t), \tag{A21}$$

eqn (A20) can be simplified to a Fredholm integral equation of the second kind. The contact problem stated in (1)–(3) has now been reduced to the integral equation stated in (6).